J. Fluid Mech. (1970), *vol.* 44, *part* 3, *pp.* 589–603
Printed in Great Britain

Relation of turbulent mass transfer to a wall at high Schmidt numbers to the velocity field

By KAMALESH K. SIRKAR† AND THOMAS J. HANRATTY

Department of Chemistry and Chemical Engineering, University of Illinois, Urbana, Illinois

(Received 4 September 1969 and in revised form 24 March 1970)

Turbulent mass transfer to a wall at high Schmidt numbers is controlled by the velocity field within the viscous sublayer. Measurements have been obtained of the root-mean-square fluctuating mass transfer coefficient and the frequency spectrum of the fluctuating mass transfer coefficient for a Schmidt number of about 2300. From an order-of-magnitude analysis it is concluded that flow fluctuations in the direction of mean flow have little effect on the mass transfer fluctuations. A comparison of the mass transfer spectrum with the spectrum of the component of the velocity gradient in the transverse direction s_z reveals that the high-frequency portion of the s_z spectrum is not effective in transferring mass. Approximate relations between the mass transfer spectrum and the s_z spectrum are developed for high frequencies and for low frequencies.

1. Introduction

Mass transfer between a turbulent fluid and a solid wall at a high Schmidt number, S, produces a very thin concentration boundary layer in the fluid. For example, Lin, Moulton & Putnam (1953) measured concentration profiles of cadmium ion [$S = 900$] when depositing cadmium on one wall of a channel through which the fluid was flowing. They found that all of the concentration change occurred within the viscous sublayer. One concludes from such measurements that the turbulent exchange of mass between a fluid and a solid surface at high Schmidt numbers is related to the fluctuating velocity field within the viscous sublayer. This paper describes experimental and theoretical studies aimed at defining this relation. The results should be of interest not only because they contribute to our understanding of turbulent mass transfer but also because they might give some insight on how to model turbulent flow close to a wall.

The system considered is fully-developed turbulent flow in a 7·625 in. diameter pipe. An electrochemical reaction is carried out on the wall of a section of nickel pipe under conditions such that it is controlled by the rate of mass transfer. This test section is long enough that the concentration boundary layer is developed fully. The Schmidt number for the system studied varied from 2240 to 2410. A nickel wire is embedded in, and ground flush with, the wall of the test section

† Present address: Uniroyal Research Center, Wayne, New Jersey.

near its outlet. This wire is insulated from the rest of the mass transfer section so that the electric current flowing through it is proportional to the local rate of mass transfer per unit area, N. A local instantaneous mass transfer coefficient K can be defined as $K = N/(C_b - C_w)$, where C_b and C_w are the concentrations of the reacting species in the bulk and at the wall. If the reaction at the electrode is fast enough $C_w \cong 0$ and fluctuations in the current are directly related to fluctuations in K. Measurements have been made of the time-averaged mass transfer coefficient $\overline{K}$, the mean-squared value of the fluctuations in the mass transfer coefficient $\overline{k^2}$ and the spectral density function of the fluctuations in the mass transfer coefficient $W_k(n)$, where n is frequency in cycles per second. An analysis is presented which relates $\overline{K}$, $\overline{k^2}$ and $W_k(n)$ to measurements of the properties of the fluctuating shear stress at the wall by Mitchell & Hanratty (1966), Sirkar (1969) and Sirkar & Hanratty (1970) and to studies of certain aspects of the structure of turbulence close to a wall by Kline and his co-workers (Kline, Reynolds, Schraub & Runstadler 1967; Schraub & Kline 1965).

The experiments are a continuation of work in a 1 in. pipe by Shaw & Hanratty (1964). The interpretation of these previous experiments was handicapped because the very small scale of k in the transverse direction caused averaging over the test electrode. Shaw & Hanratty estimated $\overline{k^2}$ by carrying out measurements with electrodes of different size and by extrapolating these measurements to an electrode of zero size. The use of a 7·625 in. pipe in the recent research gave much better resolution so that it was possible to measure directly the local value of k. It has been found that the extrapolation procedure used by Shaw & Hanratty leads to considerable error.

2. Order-of-magnitude analysis

An order-of-magnitude analysis of the mass balance equations similar to that done by Shaw & Hanratty (1964) will first be performed. It is found that the fluctuating concentration field is governed primarily by flow fluctuations perpendicular to the wall and transverse to the direction of mean flow. A greatly simplified version of the mass balance can then be derived.

The concentration of the species being transferred normalized with respect to the bulk concentration at the entrance to the mass transfer section is designated as $C^+ = C/C_{b0}$. The time-averaged dimensionless concentration is designated as $\overline{C^+}$. The concentration fluctuations c^+ are defined as $C^+ = \overline{C^+} + c^+$. Because of symmetry $\overline{C^+}$ does not vary in the circumferential direction. Since the concentration profile is fully developed, $\overline{C^+}$ varies linearly with distance in the direction of mean flow x. From a mass balance it is found that

$$\frac{\partial \overline{C}}{\partial x} = \frac{\partial C_b}{\partial x} = \frac{4\overline{N}}{U_b d}, \tag{1}$$

where d is the pipe diameter and U_b is the bulk-averaged velocity. From the measured values of $\overline{N}$ it is concluded that $\partial C_b/\partial x$ was negligible over the length of the mass transfer section.

The velocity components in the x direction, in the direction perpendicular to the wall y and in the z direction are normalized with respect to the friction velocity u^* and are designated by U^+, V^+ and W^+. Since the flow is fully developed only the time-averaged value of U is non-zero. Therefore $\overline{V} = 0$ and $\overline{W} = 0$. Fluctuating velocity components u^+, v^+ and w^+ are defined by the equations

$$U^+ = \overline{U^+} + u^+, \quad V^+ = \overline{V^+} + v^+, \quad W^+ = \overline{W^+} + w^+, \tag{2}$$

and are related through the equation of conservation of mass

$$\frac{\partial u^+}{\partial x^+} + \frac{\partial v^+}{\partial y^+} + \frac{\partial w^+}{\partial z^+} = 0. \tag{3}$$

Here the co-ordinates have been made dimensionless using a length defined in terms of the kinematic viscosity ν and the friction velocity.

A mass balance yields an equation for C^+:

$$\frac{\partial C^+}{\partial t^+} + \overline{U}^+ \frac{\partial C^+}{\partial x^+} + u^+ \frac{\partial C^+}{\partial x^+} + v^+ \frac{\partial C^+}{\partial y^+} + w^+ \frac{\partial C^+}{\partial z^+} = \frac{1}{S}\left(\frac{\partial^2 C^+}{\partial x^{+2}} + \frac{\partial^2 C^+}{\partial y^{+2}} + \frac{\partial^2 C^+}{\partial z^{+2}}\right), \tag{4}$$

where the time has been made dimensionless with respect to u^* and ν. From the measurements to be presented in the paper it is found that $(\overline{k^2})^{\frac{1}{2}}/\overline{K} \cong 0{\cdot}3$. Therefore $c^+ \sim 0{\cdot}3\overline{C}^+$. From (1), $\partial \overline{C}^+/\partial x^+ = 4\overline{K}^+/R \sim 10^{-7}$, where $R = dU_b/\nu$ and $\overline{K}^+ = \overline{K}/u^*$. The instantaneous concentration gradient in the direction of mean flow is determined primarily from the fluctuating concentration field. Shaw & Hanratty (1964) reported a dimensionless integral scale for k in the x direction, Λ^+_{kx}, of approximately 350. The following estimate can therefore be made, if we assume that the magnitude of $\partial c^+/\partial x^+$ is given as c^+/Λ^+_{kx}:

$$\overline{U}^+ \frac{\partial C^+}{\partial x^+} \sim \overline{U}^+ \frac{\partial c^+}{\partial x^+} \sim \overline{U}^+ \frac{0{\cdot}3}{350} \overline{C}^+. \tag{5}$$

From measurements of the fluctuating wall shear stress obtained by Mitchell & Hanratty (1966), by Sirkar (1969), and by Sirkar & Hanratty (1970), $u^+ \sim 0{\cdot}30$–$0{\cdot}35\overline{U}^+$ and $w^+ \sim 0{\cdot}09\overline{U}^+$. From the measurements of the effect of the size of the electrode on the intensity of the mass transfer fluctuations presented in this paper we have roughly estimated that the integral scale of the mass transfer fluctuations in the z direction is given as $\Lambda^+_{kz} \cong 6{\cdot}7$. We can therefore assign the following orders of magnitude:

$$u^+ \frac{\partial C^+}{\partial x^+} \sim \overline{U}^+ \frac{0{\cdot}3 \times 0{\cdot}32}{350} \overline{C}^+, \tag{6}$$

$$w^+ \frac{\partial C^+}{\partial z^+} \sim \overline{U}^+ \frac{0{\cdot}3 \times 0{\cdot}09}{6{\cdot}7} \overline{C}^+, \tag{7}$$

One concludes from (5), (6) and (7) that $u^+ \partial C^+/\partial x^+$ and $\overline{U}^+ \partial C^+/\partial x^+$ can be neglected compared to $w^+ \partial C^+/\partial z^+$. Because of the thinness of the concentration boundary layer in the limit of large Schmidt numbers we neglect $\partial^2 C^+/\partial x^{+2}$ and $\partial^2 C^+/\partial z^{+2}$ compared to $\partial^2 C^+/\partial y^{+2}$ and as a consequence of (5), (6) and (7) we obtain the following simplified version of (4):

$$\frac{\partial C^+}{\partial t^+} + v^+ \frac{\partial C^+}{\partial y^+} + w^+ \frac{\partial C^+}{\partial z^+} = \frac{1}{S} \frac{\partial^2 C^+}{\partial y^{+2}}. \tag{8}$$

For very large Schmidt numbers the concentration boundary layer is so thin that only the limiting behaviour of the flow field as $y^+ \to 0$ need be considered. Sirkar & Hanratty (1970) showed that as $y^+ \to 0$

$$w^+ = y^+ s_z^+(z^+, t^+). \tag{9}$$

An expression for v^+ can be obtained from the equation of conservation of mass. From Mitchell & Hanratty's measurements the dimensionless x and z scales of the components of the fluctuating wall shear stress in the direction of flow are $\Lambda_{xu}^+ \cong 480$ and $\Lambda_{zu}^+ \cong 12$. Since measurements of Λ_{zw}^+ are not available, it will be assumed that $\Lambda_{zw}^+ \cong \Lambda_{zu}^+$. One therefore finds

$$\frac{\partial u^+}{\partial x^+} \sim \frac{0{\cdot}32}{480}\,\overline{U}^+, \quad \frac{\partial w^+}{\partial z^+} \sim \frac{0{\cdot}09}{12}\,\overline{U}^+. \tag{10), (11}$$

From (10) and (11) $\partial w^+/\partial z^+ \gg \partial u^+/\partial x^+$ so that (3) can be simplified to

$$\frac{\partial v^+}{\partial y^+} + \frac{\partial w^+}{\partial z^+} = 0. \tag{12}$$

Equation (12) can be integrated to give

$$v^+ = -\tfrac{1}{2} y^{+2}\, \partial s_z^+/\partial z^+. \tag{13}$$

In order to make any progress in solving (8), (9) and (13) to determine a relation between the fluctuating concentration field and the fluctuating flow field one must give some consideration to the structure of the turbulence close to the wall and to the effect of the $\partial C^+/\partial t^+$ term. An Eulerian time scale τ_E^+ is calculated as 125 from the measurements of $W_k(n)$ reported in this paper. Therefore

$$\frac{\partial C^+}{\partial t^+} \sim \frac{0{\cdot}30}{125}\,\overline{C}^+ \tag{14}$$

and cannot be neglected with respect to $w^+ \partial C^+/\partial z^+$.

It is not clear how to solve (8) analytically. Therefore, we have only tried to obtain asymptotic solutions valid for low and high frequencies.

3. The pseudo-steady-state approximation

At low frequencies one can make a pseudo-steady-state approximation whereby $\partial C^+/\partial t^+$ is neglected so that

$$w^+ \frac{\partial C^+}{\partial z^+} + v^+ \frac{\partial C^+}{\partial y^+} = \frac{1}{S} \frac{\partial^2 C^+}{\partial y^{+2}}. \tag{15}$$

One might expect that this equation describes the role of the large eddy structure which is controlling the average transfer rate to the surface. Therefore, in order to integrate (15), some assumptions need to be made about the turbulence structure close to a wall.

Recent studies by Kline *et al.* with hydrogen bubble techniques indicate the presence of 'spatially well-organized' time-dependent motions in the viscous sublayer. Definite regions of fluid updrafts have been identified at which the

flow in the x direction assumes very low values. These updraft regions have been observed to be separated from each other by a non-dimensional distance (in wall parameters) in the z direction of $\lambda^+ = 75$–105 for $0 \leqslant y^+ \leqslant 7$. Schraub & Kline (1965) have reported measurements of the instantaneous profiles of the u-velocity component and the w-velocity component which showed a regular, almost sinusoidal, z dependence. Now if we assume that w^+ can be represented by a Gaussian distribution, it can be shown that the

$$\text{Expected number of zeros per length} = \left[\frac{\int_0^\infty \gamma^+ \Gamma(\gamma^+)\, d\gamma^+}{\int_0^\infty \Gamma(\gamma^+)\, d\gamma^+}\right]^{\frac{1}{2}}, \tag{16}$$

where $\gamma^+ = 2\pi/\lambda^+$ and $\Gamma(\gamma^+)$ is the wave-number spectrum of w^+ (Rice 1954). The wave-number spectrum can be calculated from correlation function ψ_{w^+}; however, no such measurements are available. It will be assumed that ψ_{w^+} is given by the function

$$\psi_{w^+} = \overline{w^{+2}} \exp(-\pi z^{+2}/4\Lambda_{zw}^{+2}). \tag{17}$$

Then

$$\Gamma = 4\overline{w^{+2}}\,\Lambda_{zw}^+ \exp(-4\pi\Lambda_{zw}^{+2}\gamma^{+2}) \tag{18}$$

and the expected number of zeros per unit length is $1/(2\pi)^{\frac{1}{2}}\Lambda_{zw}^+$. Therefore the following approximate relation is obtained between the wavelength λ^+ and the scale Λ_{zw}^+:

$$\lambda^+ = 5{\cdot}025\Lambda_{zw}^+. \tag{19}$$

Mitchell & Hanratty (1966) found that the scale of the u-velocity component in the z direction Λ_{zu}^+ is between 11·5 and 14·0. If it is assumed that $\Lambda_{zw}^+ \cong \Lambda_{zu}^+$ then the estimate of $\lambda^+ \cong 58$–70 is in rough agreement with the measured distance between updrafts given by Schraub & Kline (1965), $\lambda^+ \cong 75$–105. It is felt that the visual observations of Kline *et al.* are a more accurate measurement of λ^+ than that estimated from the scale measurements of Mitchell & Hanratty (1966). A value of $\lambda^+ = 100$ will be used in this paper since it is the one that has been used in the most recent report by Kline *et al.* (1967).

On the basis of these measurements it is postulated that close to the wall the large-scale aspects of the w-velocity field can be represented by the periodic structure shown in figure 1. The dimensionless distance between updrafts λ^+ is twice the distance between the zeros of w.

Equation (15) can be integrated (Lighthill 1950) using (9) and (13) for v^+ and w^+ and the boundary conditions $C^+ = 1$ for $y^+ \to \infty$ and $C^+ = 0$ for $y^+ = 0$ to give the following equation for the local instantaneous value of the mass transfer coefficient:

$$K^+ = \frac{(S)^{-\frac{2}{3}}(9)^{-\frac{1}{3}} s_z^{+\frac{1}{2}}(z^+, t^+)}{\Gamma(\frac{4}{3})\left[\int_{z_0^+}^{z^+} s_z^{+\frac{1}{2}}(q^+, t^+)\, dq^+\right]^{\frac{1}{3}}}, \tag{20}$$

where $\Gamma(\frac{4}{3})$ is the gamma function. Here z_0^+ refers to a location in figure 1 where $w^+ = 0$ and the fluid is impinging on the solid boundary.

In accordance with the eddy model shown in figure 1 we can define $s_z^+(z^+, t^+)$ by the equation

$$w^+ = s_z^+(z^+, t^+)\, y^+ = w_1^+(t^+)\, b(\gamma^+ z^+)\, y^+, \tag{21}$$

where $b(\gamma^+ z^+)$ could be a simple sine wave or a more complicated periodic function. If (21) is substituted into (20) and z_0^+ is taken as zero the following relation is obtained for K^+:

$$K^+ = g a(\gamma^+ z^+)\, \gamma^{+\frac{1}{3}} |w_1^+(t^+)|^{\frac{1}{3}}. \tag{22}$$

Here

$$g = \frac{S^{-\frac{2}{3}}}{(9)^{\frac{1}{3}}\, \Gamma(\frac{4}{3})} \tag{23}$$

and

$$a(\gamma^+ z^+) = \frac{b^{\frac{1}{2}}(\gamma^+ z^+)}{\left[\int_0^{\gamma^+ z^+} b^{\frac{1}{2}}(\gamma^+ q^+)\, d(\gamma^+ q^+)\right]^{\frac{1}{3}}}. \tag{24}$$

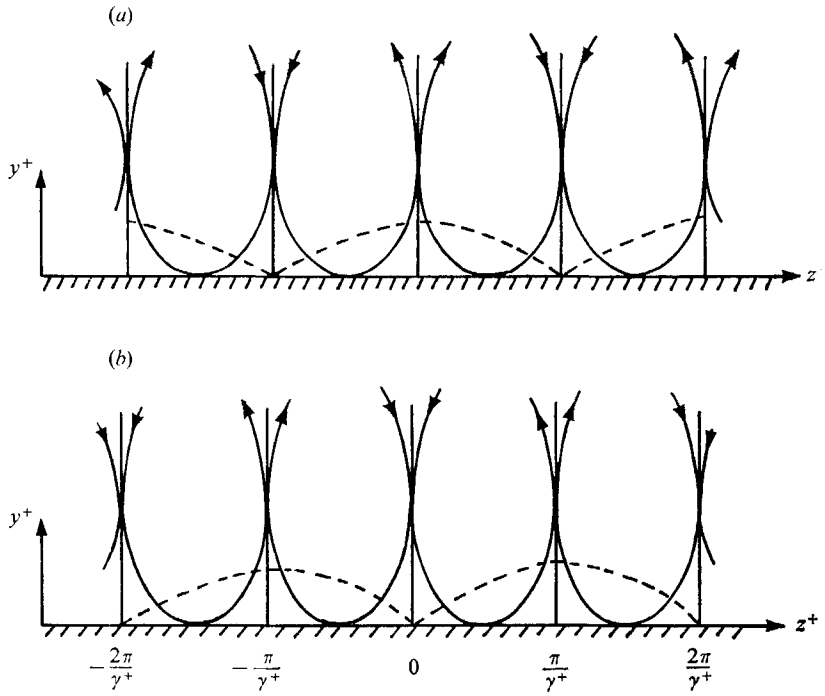

FIGURE 1. Model of large eddies. – – – –, concentration boundary layer. (*a*) $w_1^+(t^+) < 0$. (*b*) $w_1^+(t^+) > 0$.

Since K^+ is always positive and since the direction of w^+ may change we use the absolute value $w_1^+(t^+)$ in (22).

The time-averaged mass transfer coefficient is given as

$$\overline{K}^+ = \gamma^{+\frac{1}{3}} g \langle a(\gamma^+ z^+) \rangle\, E[|w_1^+(t^+)|^{\frac{1}{3}}], \tag{25}$$

where $E[|w_1^+(t^+)|^{\frac{1}{3}}]$ is the expected value of $|w_1^+(t^+)|^{\frac{1}{3}}$ and $\langle a(\gamma^+ z^+) \rangle$ is the space average of $a(\gamma^+ z^+)$:

$$\langle a(\gamma^+ z^+) \rangle = \frac{1}{\pi} \int_0^{\pi} \frac{b^{\frac{1}{2}}(\gamma^+ z^+)\, d(\gamma^+ z^+)}{\left[\int_0^{\gamma^+ z^+} b^{\frac{1}{2}}(\gamma^+ q^+)\; d(\gamma^+ q^+)\right]^{\frac{1}{3}}}. \tag{26}$$

For $b(\gamma^+z^+) = \sin\gamma^+z^+$,

$$\langle a(\gamma^+z^+)\rangle = 0{\cdot}854. \tag{27}$$

Sirkar & Hanratty (1970) have found that the probability distribution function for s_z is roughly described by a Gaussian distribution. It will be assumed that the probability distribution for w_1^+ is also Gaussian:

$$P[w_1^+(t^+)] = \frac{1}{(2\pi)^{\frac{1}{2}}\sigma}\left[\exp -\frac{w_1^{+2}(t^+)}{2\sigma^2}\right], \tag{28}$$

where

$$\sigma^2 = \overline{w_1^{+2}(t^+)}. \tag{29}$$

It follows from (25) and (28) that

$$\bar{K}^+ = \frac{2^{\frac{1}{6}}\langle a(\gamma^+z^+)\rangle\gamma^{+\frac{1}{3}}\sigma^{\frac{1}{3}}\Gamma(\frac{2}{3})S^{-\frac{2}{3}}}{(9)^{\frac{1}{3}}\Gamma(\frac{4}{3})\pi^{\frac{1}{2}}}. \tag{30}$$

Thus according to the pseudo-steady-state approximation, as developed here, the average mass transfer coefficient varies as $S^{-\frac{2}{3}}$. This result implies $\overline{vc} \sim y^3$ (Sirkar & Hanratty 1969). It arises because of the representation of the y dependency of w^+ by (9) and because the model for the large eddies yields a non-zero correlation between $\partial c/\partial y$ and $\partial s_z/\partial z$. If some other function had been used, a different dependency on Schmidt number would have been obtained. For example, if it were assumed that w^+ varied as y^{+2} the model would have predicted that $\bar{K}^+ \sim S^{-\frac{3}{4}}$. It is also seen that the pseudo-steady-state approximation predicts that $\bar{K}^+$ is related to the properties of the turbulence through the parameters γ^+ and σ. The parameter σ is a property of the spectrum function describing s_z. It is less than the value calculated from the intensity $\overline{s_z^2}$ since only the large eddies control the rate of mass transfer.

According to the pseudo-steady-state model the intensity of the fluctuations in the transfer coefficient is given as

$$\overline{k^{+2}} = \{g^2\langle a^2(\gamma^+z^+)\rangle\gamma^{+\frac{2}{3}}E[|w_1^+(t^+)|^{\frac{2}{3}}]\} - \{g^2\langle a(\gamma^+z^+)\rangle^2\gamma^{+\frac{2}{3}}E^2[|w_1^+(t^+)|^{\frac{1}{3}}]\}, \tag{31}$$

where $\langle a^2(\gamma^+z^+)\rangle$ is the space average of $a^2(\gamma^+z^+)$. If $w_1^+(t^+)$ is defined by a Gaussian distribution the following result is obtained by (31) and (30):

$$\frac{\overline{k^{+2}}}{\bar{K}^{+2}} = 1{\cdot}087\frac{\langle a^2(\gamma^+z^+)\rangle}{\langle a(\gamma^+z^+)\rangle^2} - 1. \tag{32}$$

If $\langle a^2(\gamma^+z^+)\rangle/\langle a(\gamma^+z^+)\rangle^2 = 1{\cdot}0$ the mass transfer intensity $(\overline{k^{+2}})^{\frac{1}{2}}/\overline{K^+}$ is estimated as 0·30. If $b(\gamma^+z^+) = \sin\gamma^+z^+$ the mass transfer intensity is estimated as 0·44.

A relation between the spectral density functions for mass transfer, $W_k(n)$, and for the w-velocity component, $W_{s_z}(n)$, can also be calculated from the pseudo-steady-state model. For this purpose it is assumed that the large eddy structure shown in figure 1 is stationary. The instantaneous mass transfer coefficient at a point z^+ in an eddy is

$$\left.\begin{aligned} K^+ &= a(\gamma^+z^+)[g\gamma^{+\frac{1}{3}}][w_1^+(t^+)]^{\frac{1}{3}} && \text{for} \quad w_1^+(t^+) > 0,\\ K^+ &= 0 && \text{for} \quad w_1^+(t^+) = 0,\\ K^+ &= a_1(\gamma^+z^+)[g\gamma^{+\frac{1}{3}}][-w_1^+(t^+)]^{\frac{1}{3}} && \text{for} \quad w_1^+(t^+) < 0, \end{aligned}\right\} \tag{33}$$

where $a(\gamma^+z^+)$ is given by (24) and

$$a_1(\gamma^+z^+) = \frac{b^{\frac{1}{2}}(\pi - \gamma^+z^+)}{\left[\int_0^{\pi-\gamma^+z^+} b^{\frac{1}{2}}(\gamma^+q^+)\,d(\gamma^+q^+)\right]^{\frac{1}{3}}}. \tag{34}$$

The observed variation of w^+ with time close to the wall is highly irregular. Therefore the procedure that has been taken is to assume that $w_1^+(t^+)$ is given by a Gaussian distribution and to use the methods presented by Davenport & Root (1958) for full-wave non-linear νth law devices of communication engineers to calculate the spectrum. Details are to be found in a thesis by one of the authors (Sirkar 1969).

One objection to the use of equations (33) is that they predict $K^+ = 0$ when $w_1^+(t^+)$ is zero. Zero instantaneous values of K^+ have not been observed in our experiments. In order to examine this effect more closely the time variation of K^+ has been calculated for the case where $b(\gamma^+z^+)$ is given by a sine function. As shown in figure 2 the region over which K^+ is predicted to have values close to zero is very small.

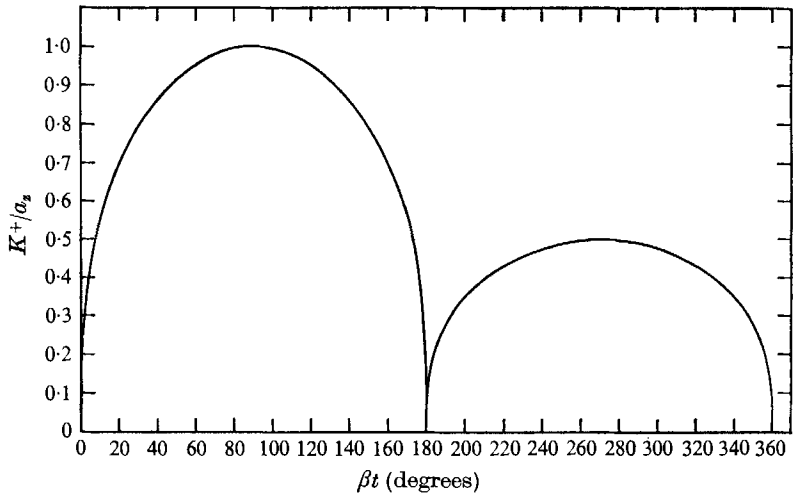

FIGURE 2. Time variation of K due to a sinusoidal varying w velocity. Location $yz^+ = 0{\cdot}5585$ radians. $w_1^+(t) = A_s \sin \beta t$; $K^+ = a_2(\sin \beta t)^{\frac{1}{3}}$, $0 \leqslant \beta t \leqslant \pi$; $K^+ = a_3(-\sin \beta t)^{\frac{1}{3}}$, $\pi \leqslant \beta t \leqslant 2\pi$.

4. Linear model of the concentration field

The following linearized form of the mass balance equation can be derived for the concentration fluctuation c^+:

$$\frac{\partial c^+}{\partial t^+} + v^+ \frac{\partial \bar{C}^+}{\partial y^+} = \frac{1}{\bar{S}} \frac{\partial^2 c^+}{\partial y^{+2}}. \tag{35}$$

The use of (35) to relate k^+ to the fluctuating velocity field could be justified in a number of ways. One of these is that $w^+ \partial C^+/\partial z^+$ is much smaller than the estimate given in (7). Another is that (35) is applicable only to concentration fluctuations

for which $c^+ \ll 1$. Still another is that (35) describes the effects of small disturbances on the concentration field set up by the large eddy structure treated in the previous section. Let C_s be the concentration field set up by the pseudo-steady-state model. Then a small high-frequency fluctuation could be described by the equation

$$\frac{\partial c^+}{\partial t^+} + v^+ \frac{\partial C_s^+}{\partial y^+} = \frac{1}{S} \frac{\partial^2 c^+}{\partial y^{+2}}. \tag{36}$$

If (36) is solved and the ensemble average is taken the result is quite close to the solution of (35).

The above interpretations suggest that (35) should be applicable to the high-frequency mass transfer fluctuations. A solution of (35) will be sought for harmonic fluctuations in v^+ varying as y^{+2} close to the wall:

$$v^+(y^+, t^+) = \hat{v}\, e^{i\beta^+ t^+}\, y^{+2}, \tag{37}$$

where $\beta^+ = 2\pi n^+$. The mean concentration field is taken as

$$\bar{C}^+ = \tfrac{3}{2}(y^+/\delta_c^+) - \tfrac{1}{2}(y^+/\delta_c^+)^3, \tag{38}$$

where

$$\delta_c^+ = 3/2S\bar{K}^+. \tag{39}$$

The solution of (35) is of the form

$$c^+ = \hat{c}(y^+)\, e^{i\beta^+ t^+}. \tag{40}$$

Using the boundary conditions

$$\begin{aligned} \hat{c} &= 0 \quad \text{at} \quad y^+ = 0, \\ \hat{c} &= 0 \quad \text{at} \quad y^+ = \infty, \end{aligned} \tag{41}$$

we obtain the following solution of (35):

$$\left.\begin{aligned} \hat{c} = \hat{v}S^2\overline{K^+}\Bigg(B\,e^{-my^+} &+ \frac{e^{my^+}}{2m}\left[\int_\infty^{y^+}\left\{y^{+2}e^{-my^+} - \frac{4S^2\overline{K^+}^2}{9}\,y^{+4}e^{-my^+}\right\}dy^+\right] \\ &- \frac{e^{-my^+}}{2m}\left[\int_0^{y^+}\left\{y^{+2}e^{my^+} - \frac{4S^2\overline{K^+}^2}{9}\,y^{+4}e^{my^+}\right\}dy^+\right)\Bigg), \\ B = \left[\frac{1}{m^4} + \frac{3\,e^{-3m/2S\bar{K}^+}}{2S\bar{K}^+m^3} + \frac{5\,e^{-3m/2S\bar{K}^+}}{m^4} + \frac{8S\,\bar{K}^+\,e^{-3m/2S\bar{K}^+}}{m^5}\right] \\ \text{and} \qquad m = (1+i)\,(\beta^+S/2)^{\frac{1}{2}}. \end{aligned}\right\} \tag{42}$$

The spectral density functions of the v velocity and of the mass transfer fluctuations are defined as

$$\left.\begin{aligned} W_{\hat{v}}(\beta^+) &= \hat{v}(\beta^+)\,\hat{v}^*(\beta^+) \\ \text{and} \qquad W_{\hat{k}^+}(\beta^+) &= \hat{k}(\beta^+)\,\hat{k}^*(\beta^+), \end{aligned}\right\} \tag{43}$$

where $*$ signifies the complex conjugate and β is the frequency in radians per second. From (41) we obtain the relation between $W_{\hat{v}}(\beta^+)$ and $W_{\hat{k}^+}(\beta^+)$:

$$\begin{aligned} W_{\hat{k}^+}(\beta^+) = W_{\hat{v}}(\beta^+)\Bigg[&\frac{4 + 100\,e^{-2p_1} + 40\,e^{-p_1\cos p_1}}{(\beta^{+3}S/\bar{K}^{+2})} + \frac{9\,e^{-2p_1}}{S^2\beta^{+2}} + \frac{256\bar{K}^{+4}e^{-2p_1}}{\beta^{+4}} \\ &+ \frac{6\sqrt{(2)}[e^{-p_1\sin p_1} + e^{-p_1\cos p_1} + 5\,e^{-2p_1}]}{(S^{\frac{1}{2}}\beta^{+\frac{1}{2}}/\bar{K}^+)} \\ &+ \frac{32\sqrt{(2)}[e^{-p_1\cos p_1} - e^{-p_1\sin p_1} + 5\,e^{-2p_1}]}{[\beta^{+\frac{7}{2}}S^{\frac{1}{2}}/\bar{K}^{+3}]}\Bigg], \end{aligned} \tag{44}$$

where $p_1 = (3/\bar{K}^+)(\beta^+/8S)^{\frac{1}{3}}$. For $S = 2300$, (44) simplifies to the following for $\beta^+ > 10^{-2}$:

$$W_{k^+}(\beta^+) = W_0(\beta^+)\,\overline{4K^+}^2/\beta^{+3}S. \tag{45}$$

Equation (45) is the asymptotic solution to (35) for large S. It can be obtained directly from (35) by asymptotic methods using inner and outer expansions.

5. Description of the experiments

The flow loop in which the measurements of $\bar{K}$, $\overline{k^2}$, and W_k were made is described in a previous paper (Sirkar & Hanratty 1970). It provided a symmetric fully developed turbulent flow to the 7·625 in. test section which consisted of 20 in. of brass pipe electroplated with 0·0015 in. of nickel and 18 in. of nickel pipe having a wall thickness of $\frac{3}{16}$ in. at the lowest R and of 18 in. of nickel pipe at the highest R.

The test electrodes were fabricated by inserting into the wall of the nickel pipe nickel wires having diameters of 0·0155, 0·0245, 0·0355 and 0·123 in. A $\frac{1}{8}$ in. diameter blind hole was drilled in the pipe wall until its thickness was $\frac{1}{16}$ in. Holes 0·006 in. larger than the wire diameter were drilled into the remaining thickness of nickel wall. The entire hole was filled with epoxy. After the epoxy had hardened a hole of the same size as the wire was drilled. The wire was inserted into the hole and glued in place with epoxy cement. The inside of the pipe wall was sanded smooth so as to leave the tip of the wire embedded flush with the wall and insulated from the wall. The test section and test electrode were the cathode for the electrochemical system. The anode is located downstream from the cathode and was designed so that it has an area over an order of magnitude greater than that of the cathode. It consists of a large number of nickel sheets located inside three acrylic pipes each having a length of 2 ft 3 in. and a diameter of 8·4 in.

The electrolyte pumped through the system was 0·0033 N in potassium ferrocyanide, 0·0033 N in potassium ferricyanide, and 1·94 N in sodium hydroxide. The ferricyanide ions are reduced to ferrocyanide ions at the cathode and ferrocyanide ions are oxidized to ferricyanide at the anode. The electric current flowing in the electrochemical circuit is directly proportional to the rate of reaction at the cathode. The current I flowing through the test electrode is therefore related to the rate of transfer of ferricyanide ions to a unit area of test electrode N by the equation $I = ANF$ where F is Faraday's constant and A is the area of the test electrode. For all of the test conditions, a plot of I *versus* the voltage applied to the cathode and the test electrode indicated a plateau on which I is independent of the applied voltage. By operating in this plateau region one can be assured that the concentration of ferricyanide ion at the wall is essentially zero. Under these conditions I is directly proportional to the mass transfer coefficient, $I = KAFC_b$. The temperature of the solution was controlled at 25 °C. The diffusion coefficient D for the ferricyanide was obtained from the measurements by Gordon & Tobias (1963).

Two electrode circuits were used. One of them is for the test electrode. The other is for the control electrode which generates the fully developed concentra-

tion profile. The circuit on the test electrode converts the current into a voltage at the output of an operational amplifier. The amplifier negative input connected to the electrode holds the cathode voltage constant at the value of the voltage at the positive input, which is controlled by the setting of a 1 kΩ potentiometer. A 10 pF feedback capacitor and a 500 Ω input resistance were necessary to improve closed loop stability. The value of the feedback resistance R_f varied from 14·0 kΩ to 16·4 MΩ depending on the resistance in the electrochemical circuit and the electrode size. The IR drop across R_f directly gives the current flowing through the electrochemical circuit and is determined from the amplifier output voltage. The amplifier and the circuit for the control electrode were specially designed so that currents up to 2 amperes could be handled in the feedback loop.

6. Results of experiments

Experiments were conducted over a Reynolds number range of 16,300–56,200. The measured values of $\overline{K}^+$ were in agreement with the value of $3{\cdot}52 \times 10^{-4}$ by Son & Hanratty (1967) at $S = 2400$.

Measured values of the intensity $(\overline{k^2})^{\frac{1}{2}}/\overline{K}$ for the different sizes of electrodes and for the entire range of Reynolds numbers studied are shown in figure 3 as a function of the diameter of the test electrode $2a$ made dimensionless with respect to wall parameters. The data of Shaw & Hanratty obtained in a 1 in. pipe are shown in the same plot. The decrease in intensity with increasing values of $2a^+$ is interpreted as being due to averaging over the electrode surface. From these results it is concluded that the true local value of the mass transfer intensity over the Reynolds number range investigated is as follows:

$$(\overline{k^2})^{\frac{1}{2}}/\overline{K} = 0{\cdot}29. \tag{46}$$

Shaw & Hanratty (1964) obtained a value of 0·48 for the intensity because they erroneously extrapolated their data in the manner shown by the dashed line in figure 3. This resulted from the use of an exponential function to describe the transverse component of the correlation of the mass transfer fluctuations. If a correlation function of the same form as measured by Mitchell & Hanratty (1966) for shear stress fluctuations is assumed then a curve of the general shape as shown by the data in figure 3 is predicted if the non-dimensional scale in the transverse direction is taken as

$$\Lambda_{kz}^+ \cong 6{\cdot}7. \tag{47}$$

This is somewhat larger than the value given by Shaw & Hanratty (1964) and must be regarded only as a rough estimate.

Frequency spectra measured with the smallest test electrode at Reynolds numbers of 50,300 and 17,000 are shown in figure 4. It is seen that by normalizing with the wall parameters the spectra at the two Reynolds numbers can be made to agree. The dimensionless average frequency of the mass transfer fluctuations $\langle n\nu/u^{*2}\rangle$, defined as

$$\langle n\rangle = \int_0^\infty nW_k(n)\,dn \Big/ \int_0^\infty W_k(n)\,dn,$$

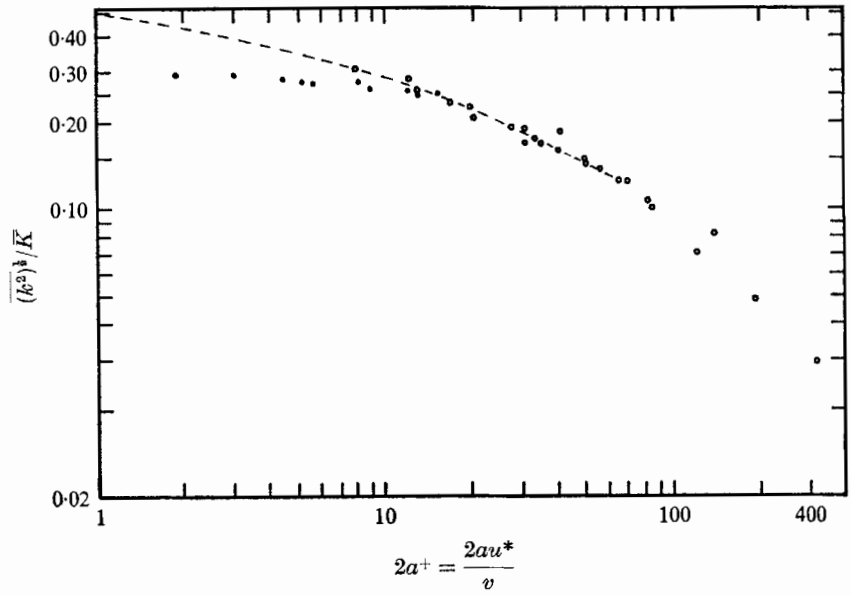

FIGURE 3. Effect of electrode size on the intensity of the mass transfer fluctuations. Wire diameter = $2a$. ●, Intensity data, $S = 2240$–2410; ○, data from Shaw & Hanratty, $S = 2400$.

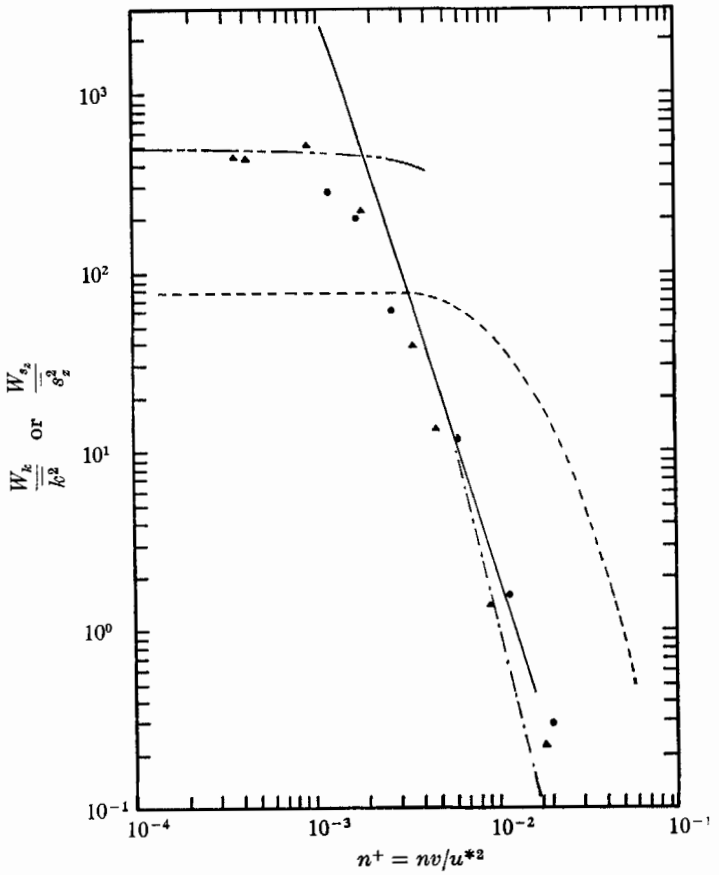

FIGURE 4. Mass transfer spectra. ●, $R = 17{,}000$, $S = 2300$, $2a^+ = 2{\cdot}0$, ▲, $R = 50{,}300$, $S = 2300$, $2a^+ = 5{\cdot}2$; —·—, linear theory using actual s_z spectrum; — · · —, pseudo-steady-state calculations; ——, linear theory using a flat s_z spectrum; - - - - -, s_z spectrum, $R = 37{,}800$.

is approximately equal to $1{\cdot}3 \times 10^{-3}$. At a Reynolds number of 50,300 this corresponds to $\langle n \rangle = 0{\cdot}28$ c/s. An Eulerian time scale τ_E^+ can be obtained from the value of the spectral density function at zero frequency. From the results in figure 4 it is estimated that

$$\tau_E^+ \simeq 125. \tag{48}$$

The frequencies of the mass transfer fluctuations were much smaller than the frequencies of the fluctuations in x or z component of the wall shear stress. For comparison, the spectral density function for the z component $W_{s_z}(n)$ obtained in a recent study by Sirkar & Hanratty (1970) at a Reynolds number of 37,800 is sketched in figure 4. The average frequency for the transverse shear stress fluctuations is about seven times as great as that for the mass transfer fluctuations.

7. Relation of mass transfer fluctuations to velocity field

The order-of-magnitude analysis presented in §2 indicated that turbulent exchange of mass is governed primarily by velocity fluctuations in the transverse direction and perpendicular to the wall. Therefore one of the interesting aspects of the results presented in the previous section is the very great difference between $W_k(n)$ and $W_{s_z}(n)$. The transfer function represented by (8) is such that high-frequency velocity fluctuations are ineffective in causing mass transfer fluctuations. For example 95% of the energy of k spectra is in a range of frequencies which contains only 40 % of the energy of the s_z spectra.

The importance of the $\partial C^+/\partial t^+$ term in (8) at high frequencies can be seen by applying the linear model. Equation (44) relates $W_{k^+}(\beta^+)$ to $W_{\hat{v}}(\beta^+)$, where it is to be noted that $2\pi W_{\hat{v}}(\beta^+) = W_{\hat{v}}(n^+)$. No measurements of the v spectra are available in the viscous sublayer. However it has been found (Sirkar & Hanratty 1970) that the spectra of both the x and the z components of the fluctuating velocity gradient at the wall have roughly the same shape. Therefore it seems reasonable to assume that $W_{\hat{v}}(n^+)$ is given by the following equation:

$$\frac{W_{s_z}(n^+)}{\overline{s_z^2}} \simeq \frac{W_{\hat{v}}(n^+)}{\overline{\hat{v}^2}}. \tag{49}$$

From Laufer's (1954) measurements we estimate that as $y^+ \to 0$

$$(\overline{v^{+2}})^{\frac{1}{2}} \simeq (\overline{\hat{v}^2})^{\frac{1}{2}} y^{+2} = 8{\cdot}0 \times 10^{-3} y^{+2}. \tag{50}$$

Therefore from (50) and our measurements of $W_{s_z}(n^+)$ and $\overline{s_z^2}$ (Sirkar & Hanratty 1970), we can estimate $W_{\hat{v}}(n^+)$. Over most of the range of frequencies of our measurements of $W_k(n)$ the spectrum for s_z is flat. Equation (45) therefore predicts that $W_k(n^+)$ should vary as $(n^+)^{-3}$ at high frequencies. This is consistent with our measurements. An actual numerical comparison between our measured $W_{k^+}(n^+)$ and the spectrum predicted from (44) and the s_z spectrum is given in figure 4. The agreement is good considering the roughness of our estimate of $W_{\hat{v}}(n^+)$. It is noted that at low frequencies the linear model diverges considerably from the measurements.

The comparison of the k spectra predicted by the pseudo-steady-state model with experiment is somewhat more complicated. The linear model relates the

value of $W_{k^+}(\beta^+)$ at a given frequency to the value of $W_b(\beta^+)$ at the same frequency. According to the pseudo-steady-state model the value of $W_k(n^+)$ at a given frequency can be influenced by the whole s_z spectrum. However since it has been found that a large portion of the $W_{s_z}(n)$ is contributing very little to the magnitude of $\overline{k^2}$ it makes sense to use only a portion of $W_{s_z}(n)$. The procedure used is to assume that the value of $\overline{K^+}$ is determined by the pseudo-steady-state model so that σ can be calculated from (30). For this purpose we took $\overline{K^+} = 3{\cdot}52 \times 10^{-4}$, $S = 2400$, $\lambda^+ = 100$ and $b(\gamma^+ z^+) = \sin \gamma^+ z^+$. From these values we obtain

$$(\overline{s_z^{+2}})_s^{\frac{1}{2}} = (\overline{w_1^{+2}})_s^{\frac{1}{2}} (\langle b^2(\gamma^+ z^+)\rangle^{\frac{1}{2}}) = 2^{-\frac{1}{2}}\sigma = 0{\cdot}047. \tag{51}$$

Here the subscript s refers to that portion of $(\overline{s_z^{+2}})^{\frac{1}{2}}$ which is contributing to the k spectrum. Sirkar & Hanratty (1970) have measured $(\overline{s_z^{+2}})^{\frac{1}{2}}$ to be 0·09, so we see that the measured $\overline{K^+}$ and the above-estimated parameters indicate that the fraction of the power in the s_z spectrum that should be used in the pseudo-steady-state model is $(0{\cdot}047/0{\cdot}09)^2$ or 27 %. Since the s_z spectrum is flat over the region of interest we will assume that

$$\begin{aligned} W_{w_1^+}(n^+) &= N \quad (0 \leqslant n^+ \leqslant n_1^+), \\ &= 0 \quad (n^+ > n_1^+), \end{aligned} \tag{52}$$

where N is obtained from the measured s_z spectra as $n^+ \to 0$ and n_1^+ is defined as

$$n_1^+ = \sigma^2/N. \tag{53}$$

From the value of σ given by (51) and the measured $W_{s_z^+}(n^+)/\overline{s_z^{+2}} \cong 70$ at low n^+ we obtain

$$n_1^+ = 3{\cdot}84 \times 10^{-3}. \tag{54}$$

About 90 % of the total power of $\overline{k^2}$ lies below this frequency.

The pseudo-steady spectrum has been calculated by Sirkar (1969) using the spectrum for the transverse velocity fluctuations given by (52) for

$$n^+ \leqslant n_1^+ = 3{\cdot}84 \times 10^{-3}$$

and is plotted as $W_k(n^+)/\overline{k^2}$ in figure 4. The calculated spectrum based on the pseudo-steady-state model is in approximate agreement with the measurements at low frequencies. It starts to become higher than the measurements at $n^+ = 1{\cdot}2 \times 10^{-3}$ and it intersects the frequency spectrum calculated from the linear model at $n^+ = 1{\cdot}8 \times 10^{-3}$. The value $\overline{k^2}$ calculated from the composite spectrum formed by using both the pseudo-steady-state spectrum and the linear spectrum up to the point of intersection is in good agreement with the measured value.

This work is supported by the National Science Foundation under Grant NSF GK–2813X.

REFERENCES

DAVENPORT, W. B. & ROOT, W. L. 1958 *An Introduction to the Theory of Random Signal and Noise*. McGraw-Hill.

GORDON, S. L. 1963 M.S. thesis, University of California, Berkeley.

KLINE, S. J., REYNOLDS, W. C., SCHRAUB, F. A. & RUNSTADLER, P. W. 1967 *J. Fluid Mech.* **30**, 741.

LAUFER, J. 1954 *NACA TR* no. 1174.

LIGHTHILL, M. J. 1950 *Proc. Roy. Soc.* A **202**, 369.

LIN, C. S., MOULTON, R. W. & PUTNAM, G. L. 1953 *Ind. Eng. Chem.* **43**, 1460.

MITCHELL, J. E. & HANRATTY, T. J. 1966 *J. Fluid Mech.* **26**, 199.

RICE, S. O. 1954 *Selected Papers on Noise and Stochastic Processes*. (Ed. N. Wax.) Dover.

SCHRAUB, F. A. & KLINE, S. J. 1965 *Rep.* MD-12, *Mech. Eng. Dept. Stanford University*.

SHAW, P. V. & HANRATTY, T. J. 1964 *A.I.Ch.E. J.* **10**, 475.

SIRKAR, K. K. 1969 Ph.D. thesis, University of Illinois.

SIRKAR, K. K. & HANRATTY, T. J. 1969 *Ind. Eng. Chem. Fund.* **8**, 189.

SIRKAR, K. K. & HANRATTY, T. J. 1970 *J. Fluid Mech.* **44**, 605.

SON, J. S. & HANRATTY, T. J. 1967 *A.I.Ch.E. J.* **13**, 689.